Science and Technology for Energy Transition **80**, 30 (2025)

https://doi.org/10.2516/stet/2025011

Innovative Strategies and Technologies for Sustainable Renewable Energy and Low-Carbon Development
Mohan Lal Kolhe and Yang Miao (Guest Editors)

Available online at:
stet-review.org

REGULAR ARTICLE OPEN ACCESS

Distributed PV auxiliary voltage control strategy in low voltage distribution network based on small AC signals

Lei Wang[1,*], Ziwei Cheng[1], Wei Zhao[1], Bo Zhang[2], Hao Zhou[1], and Zifan Li[1]

[1] State Grid Hebei Electric Power Research Institute, Shijiazhuang 050021, PR China
[2] Key Laboratory of Distributed Energy Storage and Micro-grid of Hebei Province, North China Electric Power University, Baoding 071003, PR China

Received: 3 December 2024 / Accepted: 7 March 2025

Abstract. In order to solve the problem of power flow to the distribution network and voltage overstep caused by the high proportion of distributed PV access, this paper proposes a coordinated voltage regulation strategy leveraging the reactive-active power control capabilities of PV systems. First, a systematic analysis of voltage deviation mechanisms induced by high-density PV integration is conducted. Second, a hybrid control framework is developed that synergistically coordinates reactive power compensation and active power curtailment, enabling adaptive voltage regulation across the distribution network. Third, a small-signal injection-based communication protocol is implemented to achieve decentralized coordination among multiple PV units. The simulation results demonstrate the effectiveness of the proposed strategy.

Keywords: Photovoltaic generation, Low-voltage distribution network, Out-of-limit voltage, Maximum power estimation, Small AC signal.

List of abbreviations

PV	Photovoltaic
AC	Alternating Current
RPC	Reactive Power Control
APC	Automatic Power Control
MPPT	Maximum Power Point Tracking

1 Introduction

Since the advent of industrial society, fossil fuels have been extensively exploited. As non-renewable resources, fossil fuels cause significant environmental pollution when burned. Consequently, countries around the world have been actively developing renewable energy technologies to reduce their dependence on fossil fuels [1]. According to data from the International Renewable Energy Agency (IRENA), by 2025, the global cumulative installed capacity of PV systems will reach 1860 GW, with distributed PV accounting for 32% (approximately 595 GW), becoming a core growth driver. In 2024, China's new installed capacity was 85.22 GW, accounting for about 60% of the global increase. In the same year, the United States added 36.4 GW of utility-scale PV capacity, representing approximately 58% of national total new power generation capacity [2]. Distributed photovoltaics are primarily rooftop or small-scale building systems, connected to the power grid via low-voltage lines and not subject to centralized grid dispatch. As the installed capacity of photovoltaics continues to rise, overvoltage issues have started to emerge in the low-voltage distribution network. In the low-voltage distribution network, the R/X ratio is high, and the grid voltage is influenced not only by reactive power distribution but also by active power distribution [3, 4]. When the PV power output is high due to sufficient sunlight, power backflow may occur in the distribution network, leading to an increase in voltage at the end of the line. Excessive line voltage can reduce the stability of the power grid and may lead to malfunctions in user loads near overvoltage nodes, ultimately leading to economic losses [5–7].

Various methods of voltage regulation (RPC) using reactive power have been proposed in reference [8–11] to address the overvoltage issue in the distribution network. However, the impact of reactive power on the network voltage is limited, making the use of reactive power alone for voltage regulation less effective. A method for regulating voltage (APC) by reducing active power output has been proposed. However, reducing active power can compromise the economic benefits of PV systems. In low-voltage

* Corresponding author: 13315282094@163.com

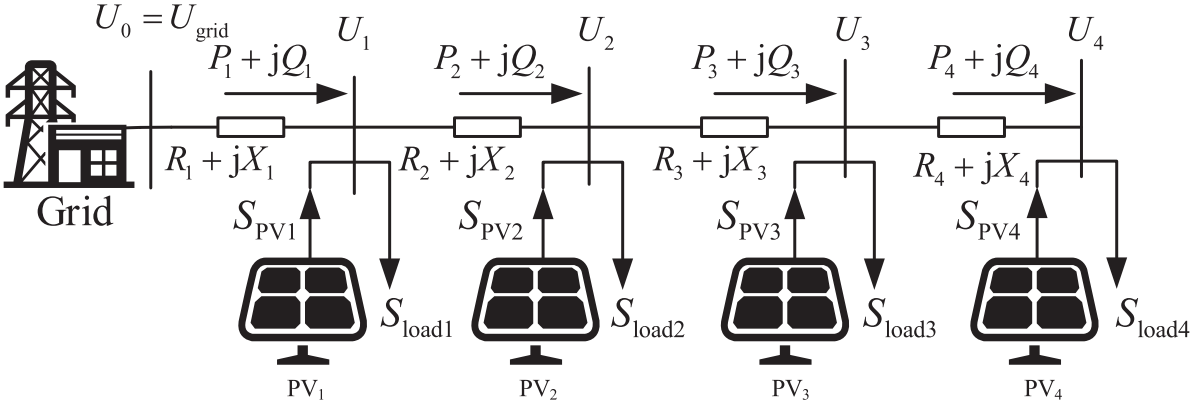

Figure 1. Distribution network with photovoltaic sources.

distribution networks, photovoltaic generation is primarily in the form of small-scale distributed systems, and a significant reduction in PV output may result in economic losses for the users of these systems [12]. Various control strategies that utilize both active and reactive power to regulate voltage are proposed. In the distribution network, overvoltage conditions often occur on lines with multiple PV power sources, with the most severe overvoltage typically occurring at the end of the line [13, 14]. The strategy is employed to ensure that the voltage at the grid connection point does not exceed the limit by reducing active power. However, the active power output of the PV system at the end of the line is reduced the most, which negatively impacts the economic interests of photovoltaic users at the line's end [13]. The coordination of multiple PV power supplies was addressed in reference [15] and [16], where a macro-control method was proposed that leverages the reactive power capacity of other photovoltaic systems to assist in voltage regulation. However, a detailed implementation strategy for coordinating the control of multiple PV power supplies was not provided. The proposed strategy is designed only for the case of a single PV power supply being connected and is not applicable to scenarios where multiple PV power supplies are installed on a single feeder line [14].

This paper proposes an auxiliary voltage regulation control strategy for photovoltaic inverters. When the grid voltage is within the normal range, the photovoltaic system operates at the maximum power point with a unit power factor. As the grid voltage increases, the photovoltaic system begins to absorb reactive power to help suppress further voltage rise. If the grid voltage continues to exceed the preset threshold, the photovoltaic system reduces its active power output to prevent the voltage from increasing further. Once the photovoltaic system reaches its regulation limit, the system transmits a signal to the next higher-level inverter. Upon receiving the signal, the upper-level inverter adjusts the set voltage in the regulation strategy to match the current grid voltage, and the process continues until all photovoltaic systems reach their regulation limits. This control strategy enables each photovoltaic inverter to actively participate in the grid's voltage regulation process while maximizing the economic benefits of each photovoltaic power source.

This paper focuses on addressing the issue of coordinated regulation of reactive and active power of PV sources and their participation in voltage adjustment of distribution networks. The proposed strategy can fully exploit the voltage support capability of PV sources, ensure the economic benefits of photovoltaic power generation, and achieve multi-machine coordinated control of distributed PV sources. Simulation examples verify the effectiveness of the proposed strategy.

2 Causes of overvoltage of distribution network caused by photovoltaic access

The typical structure of a low-voltage distribution network containing distributed PV power is shown in Figure 1.

In Figure 1, U_k represents the voltage magnitude at node k; P_k and Q_k are the active power and reactive power flowing into node k respectively; $P_{pv,k}$ and $Q_{pv,k}$ are respectively the active and reactive power emitted by the k photovoltaic power supply; $P_{load,k}$ and $Q_{load,k}$ indicate the local load at node k. The relationship between the horizontal and vertical components of voltage drops and voltage is as follows:

$$\begin{aligned} \Delta \dot{U}_k &= \frac{R_k P_k + X_k Q_k}{|\dot{U}_k|} \\ \delta \dot{U}_k &= \frac{X_k P_k - R_k Q_k}{|\dot{U}_k|} \end{aligned} \tag{1}$$

The phasor diagram showing the relationship between the node voltage and the horizontal and vertical components of the voltage drop is presented in Figure 2.

In low-voltage distribution networks, the phase angle difference between two nodes is small, and the difference in voltage amplitude is primarily influenced by the vertical component of the voltage drop, while the horizontal component can be neglected. Therefore, the voltage difference between the nodes can be expressed as:

$$|\dot{U}_{k-1}| - |\dot{U}_k| \approx \Delta \dot{U}_k = \frac{R_k P_k + X_k Q_k}{|\dot{U}_k|} \tag{2}$$

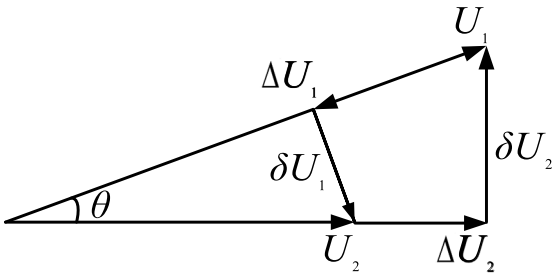

Figure 2. Voltage drop phasor diagram.

In low-voltage distribution networks, $R \gg X$ the voltage amplitude is mainly affected by the active power distribution. When line losses are neglected, the active power flowing into the k node can be expressed as:

$$P_k = P_{\text{load},k} + P_{k+1} - P_{\text{pv},k} \tag{3}$$

When sunlight is sufficient, the power generated by the photovoltaic system significantly exceeds the local load, $P_{\text{pv}} \gg P_{\text{load}}$ the active power is transmitted from the end of the line to the grid, become:

$$P_k \approx -P_{\text{pv},k} + \sum_{i=k+1}^{n} -P_{\text{pv},i} = \sum_{i=k}^{n} (-P_{\text{pv},i}) \tag{4}$$

After neglecting line losses, the voltage drop formula of each node can be expressed as:

$$\left|\dot{U}_{k-1}\right| - \left|\dot{U}_k\right| \approx \Delta \dot{U}_k \approx -\frac{R_k \sum_{i=k}^{n} P_{\text{pv},i} + X_k \sum_{i=k}^{n} Q_{\text{pv},i}}{\left|\dot{U}_k\right|} \tag{5}$$

According to equation (5), under conditions of high sunlight intensity, the active power generated by the photovoltaic system significantly exceeds the local load. As a result, the voltage at the end of the distribution network becomes significantly higher than the voltage at the beginning of the line, and the end voltage will increase with the rising photovoltaic output, ultimately causing the voltage at the end of the line to exceed the limit.

3 Auxiliary voltage regulation control strategy

In low-voltage distribution networks, the R/X ratio is large, and the impact of reactive power adjustments on voltage regulation is limited. Consequently, active power regulation becomes essential for voltage control. However, reducing active power will affect the economic benefits of photovoltaic systems. According to equation (5), overvoltage at the end of the line is most severe when sunlight is abundant. If voltage control is based solely on reducing active power according to the grid voltage at the connection point, the active power output of the photovoltaic system at the end of the line will be significantly reduced, while the active power output from systems further upstream will only be slightly affected. Such a control strategy disproportionately disadvantages photovoltaic users at the line end. Therefore, photovoltaic systems need to work in coordination with each other to ensure the economic benefits of each user while maximizing the voltage regulation capabilities of each photovoltaic inverter.

The proposed strategy utilizes both reactive and active power to regulate the voltage. The strategy calculates the maximum power in real-time through maximum power estimation to ensure that each PV power source contributes 10% of the available active power to voltage regulation. Small AC signals are injected into the system to facilitate communication between the PV power sources, ensuring coordinated voltage regulation. The detailed steps are as follows.

1. When the grid voltage is within the voltage regulation dead zone, each photovoltaic power supply operates in unit power mode.
2. As the grid voltage continues to rise and exceeds the dead zone, the photovoltaic power supply initiates reactive power absorption proportional to the grid voltage.
3. When the grid voltage reaches the voltage limit, the photovoltaic power supply begins to reduce active power, unit capable of reducing up to 10% of the available active power to assist in system voltage regulation.
4. When a photovoltaic power supply reaches its adjustment limit, if the voltage continues to rise, the unit sends a signal to the previous inverter indicating that the adjustment limit has been reached. Upon receiving the signal, the last photovoltaic power supply will set the current grid voltage as the reference voltage for the voltage control strategy to participate in system voltage regulation.

3.1 Reactive power control strategy

The reactive power control strategy employs Q-U droop control, with the voltage amplitude at the grid connection point serving as the reference. The reactive power output of the photovoltaic inverter is determined by the voltage amplitude at the grid connection point. The relationship between reactive power and the voltage at the grid connection point is as follows:

$$Q = \begin{cases} -Q_{\max}, & U \geq U_{\text{limit,up}} \\ -\dfrac{Q_{\max}(U - U_{\text{dz,up}})}{U_{\text{limit,up}} - U_{\text{dz,up}}}, & U_{\text{limit,up}} > U > U_{\text{dz,up}} \\ 0, & U_{\text{dz,up}} \geq U \geq U_{\text{dz,low}} \\ \dfrac{Q_{\max}(U_{\text{dz,low}} - U)}{U_{\text{dz,low}} - U_{\text{limit,low}}}, & U_{\text{dz,low}} > U > U_{\text{limit,low}} \\ Q_{\max}, & U \leq U_{\text{limit,low}} \end{cases} \tag{6}$$

Reactive power leads to increased losses, so a voltage dead zone is set in the Q-U control strategy to optimize economic

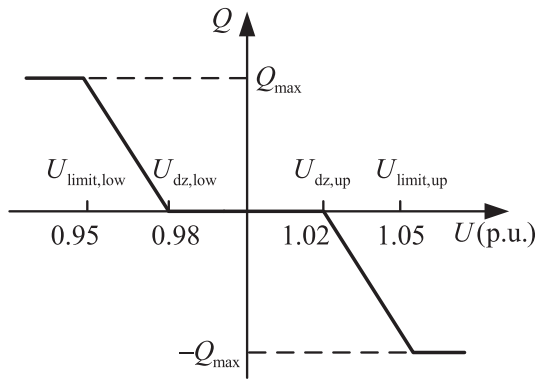

Figure 3. The relationship between reactive power and voltage emitted by photovoltaic source.

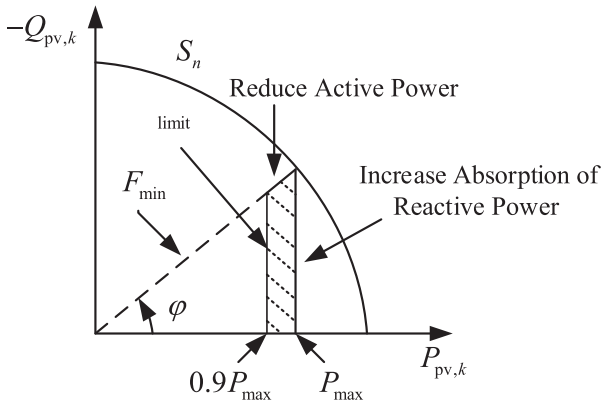

Figure 4. PV source operating range when voltage control.

benefits. When the grid voltage is within the dead zone, the photovoltaic inverter operates at unit power. Once the voltage exceeds U_{limit}, the inverter outputs the maximum reactive power. For this study, the dead zone voltage and U_{limit} are set to 1.02 and 1.05, respectively. The Q-U curve for reactive power regulation is shown in Figure 3.

The upper limit of reactive power regulation is limited by the minimum power factor of the system and the maximum capacity of the photovoltaic inverter, and 0.7 is selected as the minimum power factor in the control strategy of this paper.

$$Q_{\max} = \min\left\{|P\tan(\arccos F_{\min})|, \sqrt{S^2 - P^2}\right\} \tag{7}$$

Where $F_{\min}$ is the minimum power factor, P is the active power emitted by the current photovoltaic, S is the rated capacity of the photovoltaic inverter.

3.2 Active power control strategy

When the voltage at the grid connection point rises to U_{set} and continues to increase, the active power output must be reduced to control the voltage rise. Throughout the day, fluctuations in sunlight intensity and temperature cause corresponding variations in the power output of the photovoltaic system. At any given moment, the photovoltaic system has a maximum output power, $P_{\max}$. For example, consider the active power control strategy at a specific time: the voltage at the grid connection point is monitored. If the voltage exceeds U_{set}, the photovoltaic system reduces the output power. When the active power is reduced to $0.9P_{\max}$, the PV inverter reaches the limit of active power adjustment, corresponding to the left boundary of the shaded area in Figure 4.

The shaded area represents the operating range of the photovoltaic power supply under the control strategy described in this paper. Once the active power regulation limit is reached, if the voltage continues to rise beyond U_{set}, the photovoltaic system will send a signal to the next-level photovoltaic inverter. Take the 4-nodes in Figure 1 as an example:

$$U_4 = U_{\text{set},4} \tag{8}$$

$$\Delta U_4 = \frac{0.9R_4P_{\max} - X_4Q_{\max}}{|\dot{U}_4|} \tag{9}$$

Once the signal from the next level is detected, the system identifies that the PV power supply at the next level has reached the active power regulation limit and the point of common coupling voltage has exceeded the permissible threshold. After detecting the signal, the PV power supply takes the current point of common coupling voltage as the new U_{set}:

$$\begin{aligned} U_3 &\approx U_{\text{set},4} - \Delta U_4 \\ U_{\text{set},3} &= U_3 \end{aligned} \tag{10}$$

PV cells regulate the output power through adjustments to the operating voltage. To reduce the output power of PV cells, the operating voltage needs to be increased; to increase the output power, the operating voltage of PV cells needs to be decreased. The overall process of the active power regulation strategy is shown in Figure 5.

3.3 Maximum power estimation of photovoltaic cells

To ensure the stability of the system during normal operation, the PV power supply should work in region II. When the system voltage is normal, the PV power supply operates in the maximum power point tracking (MPPT) state, corresponding to point M in Figure 6. When the voltage exceeds Uset, the active power is continuously reduced until the active power reaches $0.9P_{\max}$, transitioning from from point M to point A in Figure 6. Upon reaching point A, the system reaches the adjustment limit.

The $\mathrm{d}P/\mathrm{d}U$ value is larger at the operating point A. To prevent large power fluctuations, two steps can be used for power reduction and MPPT as shown in Figure 5. To make the PV cell operate at point A, it is necessary to calculate the maximum power of the PV cell in real-time. The model of the PV cell is shown in Figure 7. The model is relatively simple and has high accuracy.

$$I = I_{\text{ph}} - I_0\left[\exp\left(\frac{U + IR_s}{nU_{\text{th}}}\right) - 1\right] - \frac{U + IR_s}{R_{\text{sh}}} \tag{11}$$

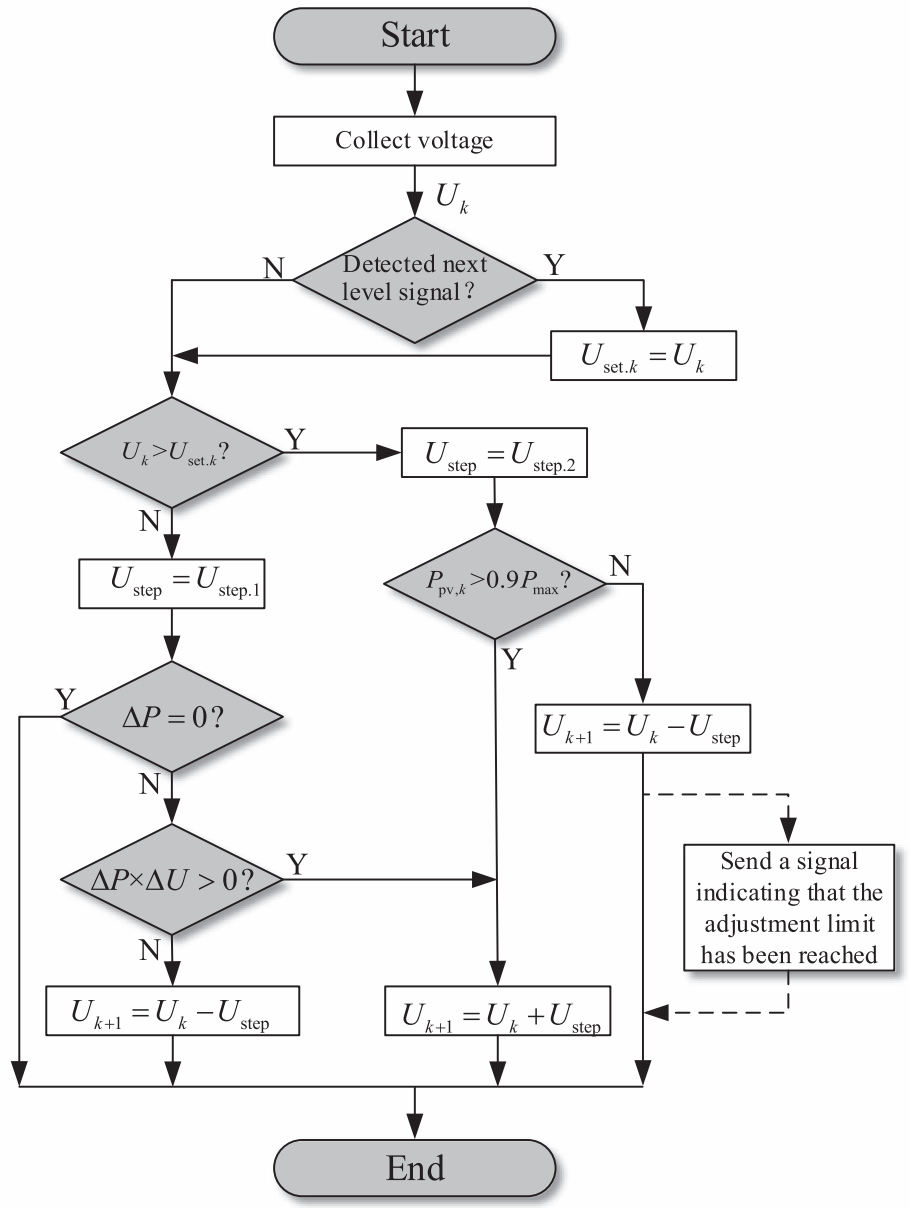

Figure 5. Active power control process.

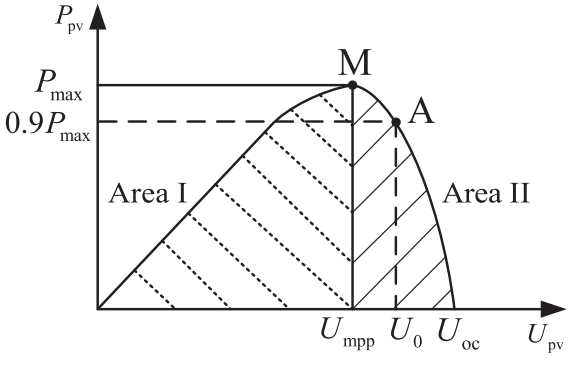

Figure 6. Photovoltaic cell P-V curve.

Where I and U are the output current and voltage of the PV cell, respectively; I_{ph} is the photo-generated current; I_0 is the reverse saturation current of the diode; n is the diode ideality factor; U_{th} is the temperature potential; R_s is series internal resistance; R_{sh} is parallel internal resistance.

Equation (11) demonstrates that the formula for calculating the maximum power is complex and computationally intensive to solve directly on a small controller. In order to simplify the calculation, the quadratic polynomial of illumination and temperature can be used to calculate the maximum power of PVs [17–19].

$$P_{max} = a_1 T + a_2 T^2 + b_1 G + b_2 G^2 + cTG + d \quad (12)$$

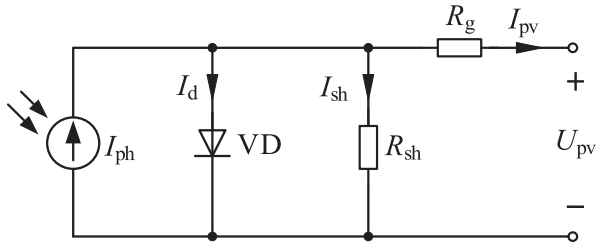

Figure 7. Equivalent circuit of photovoltaic cell.

Table 1. Parameters of PV maximum power estimation.

Parameter	Value
a_1	0.007611
a_2	−0.0008946
b_1	0.3348
b_2	-4.679×10^{-6}
c	−0.0008488
d	−4.3202

Table 2. Maximum power estimate and actual value.

Illumination intensity G/(W·m^{-2})	Temperature T/°C	Estimated power P_{max}/W	Real power P/W
400	25	119.99	119.84
800	25	243.17	242.93
1200	25	364.86	364.98
1000	15	312.97	312.97
1000	25	304.20	305.23
1000	35	295.25	295.23

Where P_{max} is the maximum output power of the PV cell under the corresponding temperature and illumination conditions; T and G are temperature and intensity of illumination, respectively. The coefficients in the equation can be derived from a linear regression analysis of the P_{max}, G and T data of the PV cells. A PV module consists of many series and parallel units. Under the assumption that the array is unobstructed, the entire module can be estimated in the same way and the total power is equal to the sum of the power of the small units. In this paper, the PV cells of type SPR-305 E-WHTD are used, and linear regression is applied to the data to derive the parameters for their maximum power estimation as shown in Table 1.

By substituting the parameters from Table 1 into equation (12), the estimated maximum power calculated by equation (12) is compared with the actual maximum power of photovoltaic cells, and the results are shown in Table 2.

Figure 8 illustrates the surface composed of the estimated power values under different illumination and temperature, and the purple points in Figure 8 represent the data from 16 PV cells used in the regression calculation. As evident from Figure 8 and Table 2, equation (12) demonstrates high accuracy in calculating the maximum power.

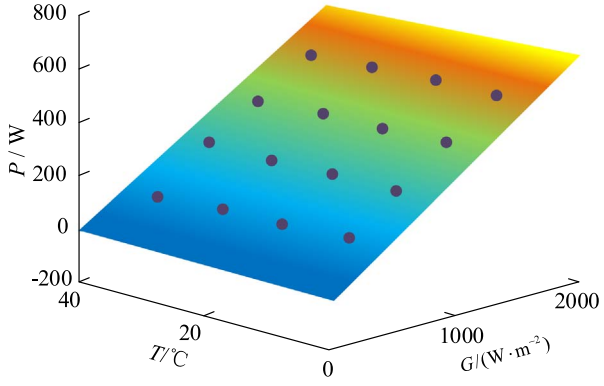

Figure 8. Surface of maximum power estimate.

3.4 Communication between inverters based on small AC signal

The auxiliary voltage regulation strategy proposed in this paper uses the power line as the transmission line of communication and achieves communication between PV inverters by injecting a small AC signal into the system.

The communication process is illustrated in Figure 9. Taking the kth PV power supply as an example, when the voltage exceeds the limit after reaching the adjustment limit, the kth PV power supply injects k small AC signals within a short period of time. When a small AC signal is detected for k times in a short time, the $k-1$th PV power supply sets $U_{set,k-1}$ to the current point of common coupling voltage value U_{k-1} according to the voltage regulation measures.

The communication strategy injects a signal into the system by superimposing a small AC signal on the original modulated wave, and only one PV power supply outputs a small AC signal at the same time. As shown in Figure 10, when any of the PV power supplies outputs a small AC signal, the other power supplies can detect the signal at the point of common coupling. The amplitude of the detected signal is the amplitude obtained by the impedance voltage divider after attenuation of the small AC signal filter. Therefore, the threshold should be comprehensively considered according to the filter and network parameters.

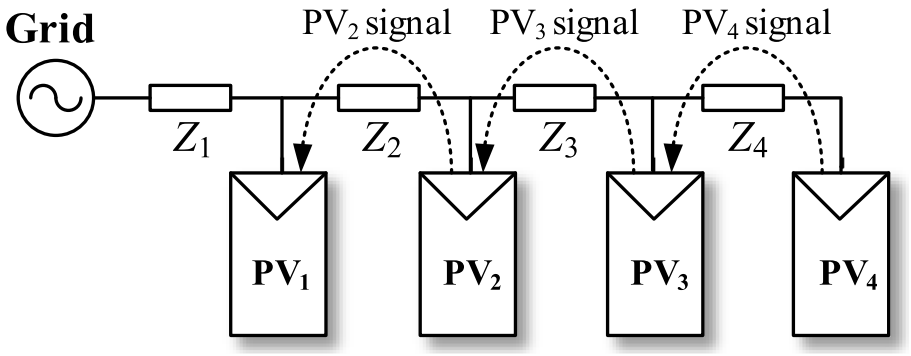

Figure 9. Information transmission process between PV sources.

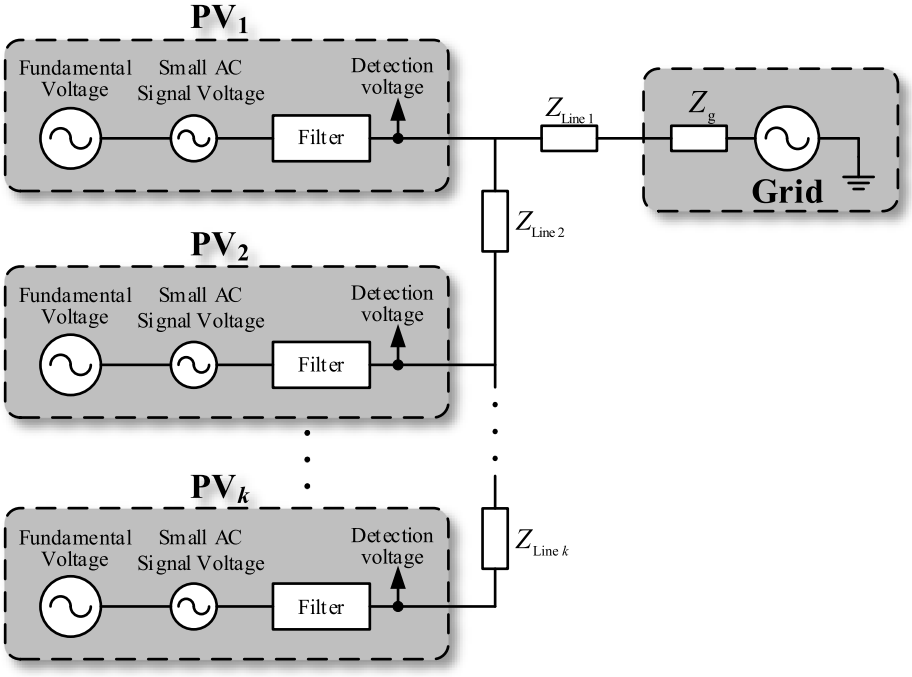

Figure 10. System simplification diagram with a small AC signal.

To avoid misjudgment and false operation caused by insufficient accuracy of the extraction algorithm during detection, the frequency of the small AC signal must be carefully selected to avoid proximity to the system's fundamental frequency. Since the points of common coupling of the PV power supplies are close to the load, the selected frequency should also avoid the harmonic frequency easily generated by some civil and industrial loads. In addition, since a filter is present on the AC side of the PV inverter, the selected small signal frequency cannot be too high. The signal frequency must be lower than the cut-off frequency of the filter rectifier on the AC side of the inverter to prevent the signal from being attenuated too much when passing through the filter. In this paper, the frequency of the small AC signal is selected as twice the fundamental frequency of 100 Hz, while the amplitude is determined based on the system's total harmonic content. Generally, the total harmonic content of the inverter should not exceed 5%, and the single harmonic content should not exceed 3% [20–21]. For the simulation, the distribution network

Table 3. Parameters of the simulation system.

Parameter	Value
Voltage levels of the power grid/V	380
Line resistance $R/(\Omega\cdot\mathrm{km}^{-1})$	0.641
Line reactance $X/(\Omega\cdot\mathrm{km}^{-1})$	0.101
Line length/m	100
PV power capacity $S/(\mathrm{kV}\cdot\mathrm{A})$	30
Small AC signal amplitude/V	5
Minimum power factor $F_{\min}$	0.7

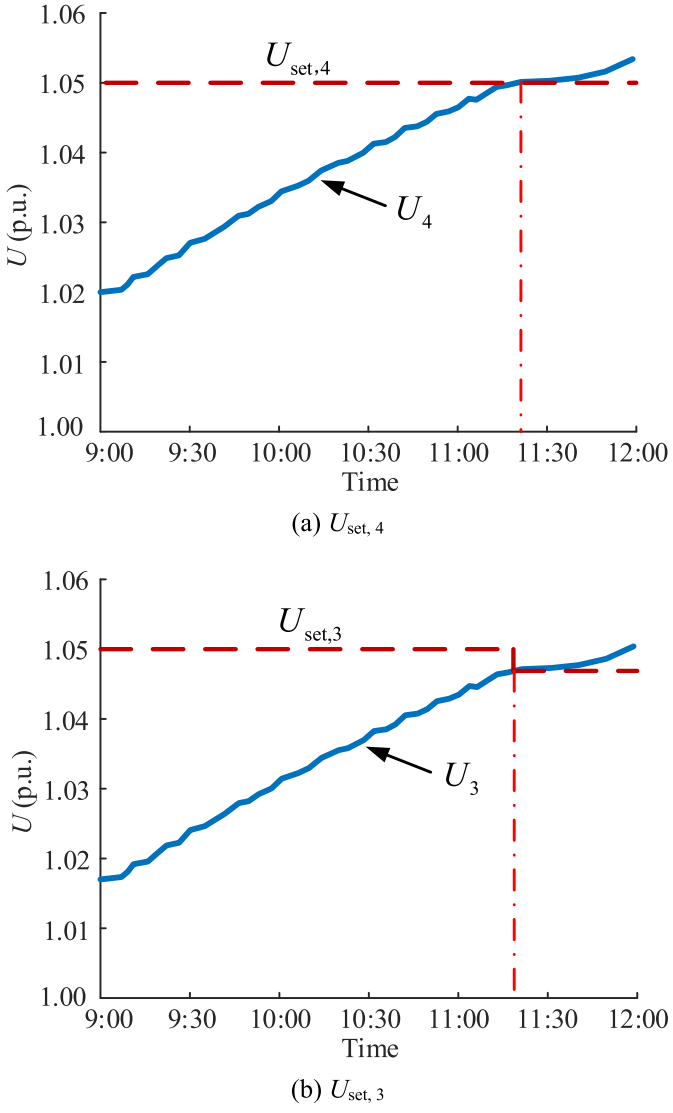

Figure 11. The voltage of grid-connection point and U_{set} of PV_4 and PV_3.

voltage amplitude is set to 311 V, and the small AC signal amplitude is selected as 5 V.

4 Simulation analysis

To validate the proposed control strategy, the topology depicted in Figure 1 is simulated on MATLAB, and the parameters used in the simulation are shown in Table 3. $PV_{1\sim4}$ have the same parameters, and the initial value of U_{set} for each PV power supply is 1.05 p.u.

As light intensity continuously increases, the active power output of the photovoltaic power supply also increases. According to equation (5), when the output power of the PV power supply increases, the voltage at each node in the Distribution network continues to increase, as shown in Figure 11. At around 11:25, the voltage at PV4 reaches the upper voltage limit of 1.05 p.u. If the PV power supply still maintains the MPPT control strategy, the voltage of each node of the distribution network will continue to rise until the node voltage exceeds the limit, and there is a voltage safety risk.

The outputs of PV_4 and PV_3 under the proposed control strategy are depicted in Figure 12 and Figure 13, respectively. The PV power supply absorbs reactive power from the grid according to equation (6) as the point of common coupling voltage U increases continuously. P_{max} is the

maximum power value estimated by the maximum power estimation method. The PV power supply remains in the MPPT state until the system reaches its regulation limit. As shown in Figure 11 and Figure 12, when the voltage U_4 exceeds $U_{set,4}$, PV_4 starts to reduce the active power in active power reduction mode. At this time, the reactive power is also reduced by the limitation of the minimum power factor of the system. Therefore, the voltage at PV4 is effectively controlled.

When $P_{pv,4}$ is equal to $0.9P_{max}$, PV_4 reaches the regulation limit, a small AC signal is injected into the system, as

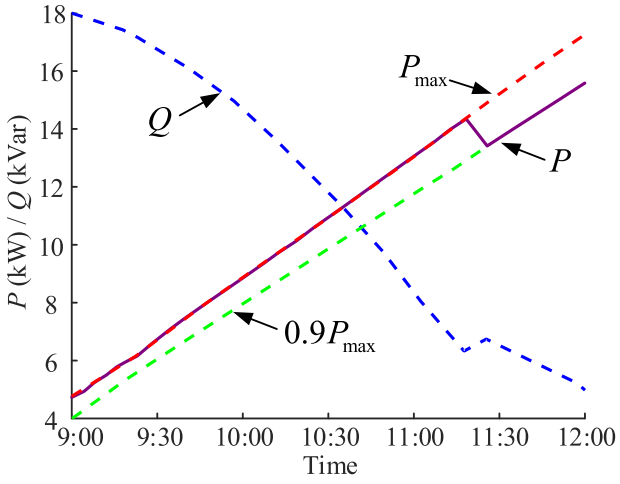

Figure 12. The active and reactive power of PV_4.

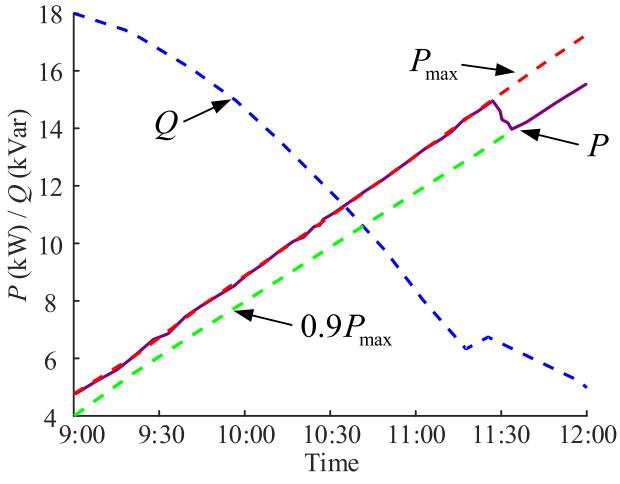

Figure 13. The active and reactive power of PV_3.

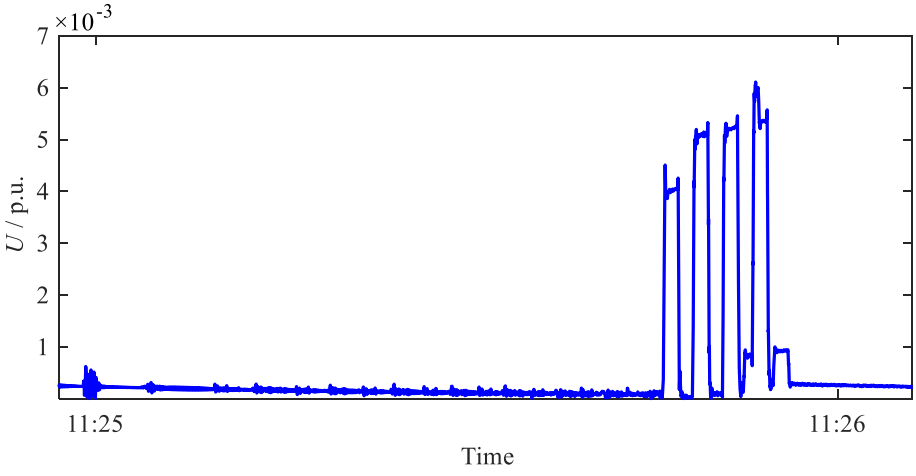

Figure 14. Small AC signal detected at PV_3.

shown in Figure 14. When PV_3 detects the small AC signal from PV_4, $U_{set,3}$ is set to the current U_3 value of 1.046 p.u. When the voltage continues to rise, PV_3 begins to reduce the active power, and enter the next regulatory process similar to PV_4.

Each PV power supply performs real-time Fourier analysis on the point of common coupling voltage to extract the 100 Hz frequency component. As shown in Figure 14, four small AC signals are detected within a short period, indicating that PV_4 has reached its regulation limit. Upon detecting these signals, PV_3 initiates a response by setting the current voltage as the new $U_{set,3}$. The active and reactive power coordination control strategy presented in this study is compared with the traditional RPC strategy. Under identical operating conditions, the voltages of each node at different times under the control of two different strategies are shown in Figure 14.

Figure 15 illustrates that reactive power regulation can effectively regulate voltage to some extent, but the voltage will still exceed the limit quickly when the PV power is high. The voltages at each node at 12:00 noon are shown in Table 4. Taking U_4 in Table 4 as an example, the grid voltage is 1.069 without control. After adding reactive power control, the grid voltage drops to 1.059, and the node voltage drops to 1.054 after 10% active power reduction by using the control strategy of this paper. After the voltage exceeds the limit, 10% active power reduction of the PV power supply significantly impacts the regulation of grid voltage.

The simulation results show that the proposed control strategy is effective in suppressing the voltage overlimit problem of high proportion PV access to the distribution network. When the photovoltaic reactive power support capacity alone cannot restrain the voltage overlimit of the distribution network nodes, other reactive power compensation measures or active power regulation means are needed at this time, and relevant research results have been obtained, which will not be described here.

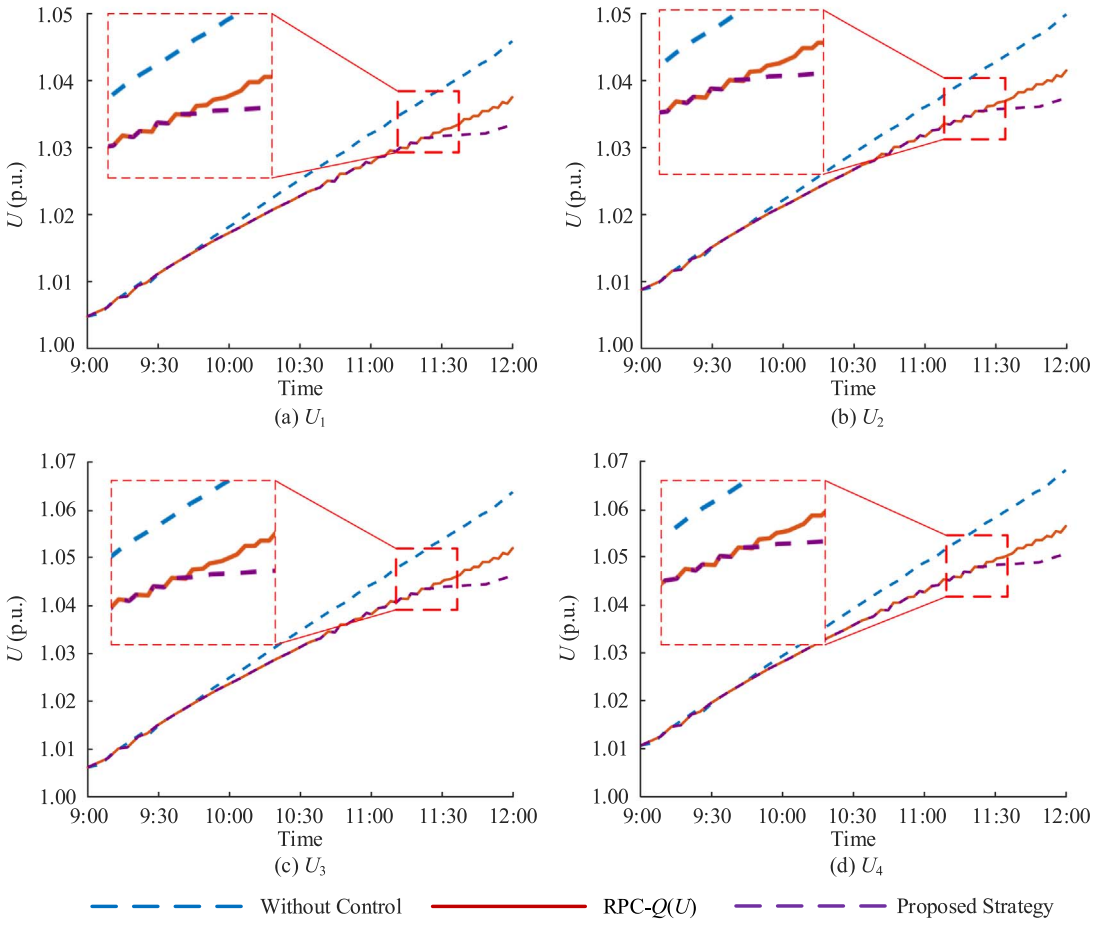

Figure 15. Node voltage under two control strategies.

Table 4. The voltage of each node at 12:00 o'clock.

Control strategy	Node voltage U_k (p.u.)			
	U_1	U_2	U_3	U_4
Without control	1.028	1.049	1.062	1.069
RPC-$Q(U)$	1.024	1.041	1.053	1.059
Proposed strategy	1.022	1.038	1.048	1.054

5 Conclusions

To address the voltage limit violation challenges in low-voltage distribution networks with high-penetration PV integration, an innovative distributed PV auxiliary voltage regulation strategy utilizing small AC signal communication is proposed. The developed control methodology optimally leverages the reactive power support capability of PV inverters while maintaining PV generation economic efficiency. Compared with conventional RPC approaches, the proposed strategy demonstrates enhanced performance in three critical aspects: (1) Comprehensive utilization of PV reactive power regulation margin across various operational scenarios; (2) Strategic active power curtailment implementation during PV surplus conditions for effective voltage rise mitigation; (3) Coordinated multi-PV control mechanism ensuring equitable active power reduction allocation and preventing control conflicts. The small AC signal-based communication architecture enables decentralized PV systems to achieve cooperative voltage regulation without requiring centralized control, effectively addressing the challenges of disordered regulation and associated economic losses in conventional autonomous control schemes.

Acknowledgments

This paper is supported by Science and technology foundation of State Grid Hebei Energy Technology Service Co. Ltd (The principal research and testing technology of fast voltage regulating device of power grid with photovoltaic power station participation, TSS2023-07).

References

1 Nathwani J., Kammen D.M. (2019) Affordable energy for humanity: a global movement to support universal clean energy access[J], *Proc. IEEE* **107**, 9, 1780–1789.
2 Wang X., Wen H., Chu G., et al. (2024) Performance quantization and comparative assessment of voltage equalizers in mismatched photovoltaic differential power processing systems[J], *IEEE Trans. Power Electron.* **39**, 1, 1656–1675.

3 Zhao Y., Zhang G., Hu W., et al. (2023) Meta-learning based voltage control for renewable energy integrated active distribution network against topology change[J], *IEEE Trans. Power Syst.* **38**, 6, 5937–5940.

4 Pierrou G., Wang X. (2021) An online network model-free wide-area voltage control method using PMUs[J], *IEEE Trans. Power Syst.* **36**, 5, 4672–4682.

5 Shayani R.A., de Oliveria M.A.G. (2011) Photovoltaic generation penetration limits in radial distribution systems [J], *IEEE Trans. Power Syst.* **26**, 3, 1625–1631.

6 León L.F., Martinez M., Ontiveros L.J., et al. (2022) Devices and control strategies for voltage regulation under influence of photovoltaic distributed generation[J], *IEEE Latin Am. Trans.* **20**, 5, 731–745.

7 Gao Y., Hu X., Yang W., et al. (2017) Multi-objective bilevel coordinated planning of distributed generation and distribution network frame based on multi-scenario technique considering timing characteristics[J], *IEEE Trans. Sustain. Energy* **8**, 4, 1415–1429.

8 Samadi A., Eriksson R., Soder L., et al. (2014) Coordinated active power-dependent voltage regulation in distribution grids with PV systems[J], *IEEE Trans. Power Deliv.* **29**, 3, 1454–1464.

9 Pukhrem S., Basu M., Conlon M.F., et al. (2017) Enhanced network voltage management techniques under the proliferation of rooftop solar PV installation in low-voltage distribution network[J], *IEEE J. Emerg. Sel. Top. Power Electron.* **5**, 2, 681–694.

10 Weckx S., Gonzalez C., Driesen J. (2014) Combined central and local active and reactive power control of PV inverters [J], *IEEE Trans. Sustain. Energy* **5**, 3, 776–784.

11 Ghosh S., Rahman S., Pipattanasomporn M. (2017) Distribution voltage regulation through active power curtailment with PV inverters and solar generation forecasts[J], *IEEE Trans. Sustain. Energy* **8**, 1, 13–22.

12 Chowdhury M.M.U.T., Hasan M.S., Kamalasadan S. (2025) A novel voltage optimization co-simulation framework for electrical distribution system with high penetration of renewables[J], *IEEE Trans. Indust. Appl.* **61**, 1, 1080–1090.

13 Gerdroodbari Y.Z., Razzaghi R., Shahnia F. (2021) Decentralized control strategy to improve fairness in active power curtailment of PV inverters in low-voltage distribution networks[J], *IEEE Trans. Sustain. Energy* **12**, 4, 2282–2292.

14 Pukhrem S., Basu M., Conlon M.F., et al. (2017) Enhanced network voltage management techniques under the proliferation of rooftop solar PV installation in low-voltage distribution network[J], *IEEE J. Emerg. Sel. Top. Power Electron.* **5**, 2, 681–694.

15 Xu X., Li Y., Yan Z., et al. (2023) Hierarchical central-local inverter-based voltage control in distribution networks considering stochastic PV power admissible range[J], *IEEE Trans. Smart Grid* **14**, 3, 1868–1879.

16 Ahmed E.E., Demirci A., Poyrazoglu G., et al. (2024) An equitable active power curtailment framework for overvoltage mitigation in PV-rich active distribution networks[J], *IEEE Trans. Sustain. Energy* **15**, 4, 2745–2757.

17 Kolakaluri V.K., Aalam M.N., Sarkar V. (2024) Sampling time modulation of a photovoltaic power tracking controller based upon real-time monitoring of converter dynamics[J], *IEEE Trans. Power Electron.* **39**, 2, 2822–2834.

18 Teng J.H., Huang W.H., Hsu T.A., et al. (2016) Novel and fast maximum power point tracking for photovoltaic generation[J], *IEEE Trans. Indust. Electron.* **63**, 8, 4955–4966.

19 Yang F., Sun Q., Han Q.L., et al. (2016) Cooperative model predictive control for distributed photovoltaic power generation systems[J], *IEEE J. Emerg. Sel. Top. Power Electron.* **4**, 2, 414–420.

20 Callegari J.M.S., de Oliveira A.L.P., Xavier L.S., et al. (2023) Voltage detection-based selective harmonic current compensation strategies for photovoltaic inverters[J], *IEEE Trans. Energy Convers.* **38**, 3, 1602–1613.

21 Liu Q., Zhang L., Zhang H., et al. (2025) Distributed secondary optimal control with fast voltage recovery and minimum generation cost for islanded DC microgrids[J], *IEEE Trans. Smart Grid* **16**, 1, 4–15.